Influence of air gap and antiscatter grid on pediatric fluoroscopy and angiography image quality

Kenneth A. Fetterly, Ph.D.
Cardiovascular Diseases, Mayo Clinic, Rochester, MN

INTRODUCTION

X-ray angiography systems are used to diagnose and treat pediatric congenital heart disease. Among the substantial variability in this patient population is that patient weight ranges from <1 kg premature infants to large adolescents. Given that the X-ray scatter to primary ratio (SPR) decreases from large to small patients, the efficacy of an air gap or antiscatter grid to mitigate scatter remains uncertain. The purpose of this work was to assess the influence of a long air gap versus an antiscatter grid for pediatric patient imaging.

METHODS

Uniform Plastic Water™ phantoms of thickness 6-24 cm were positioned at the X-ray system isocenter. A 4 mm diameter Piccolo™ (Abbott Cardiovascular, Plymouth, MN), cardiovascular closure device was positioned in the center of the phantom and used as a test object. Four conditions were tested including SID 107 vs 120 cm and non-grid vs OEM ratio 15:1 grid (r15). Test images (n=1200) were acquired using a fixed X-ray technique (0.4 mm focal spot, 56 kV, 3.4 ms, 0.3 mm Cu spectral filtration, phantom-specific mA).

The SNR of the Piccolo™ was measured using a pixel-specific, multivariate statistical observer model (PSO) 1. Using the PSO, the snr^2 of each pixel within the X-ray shadow of the PiccoloTM was estimated. Then, test object SNR^2 was calculated as the sum of the pixel-specific snr^2 estimates within the X-ray shadow of the Piccolo™.

Results were compared to the patient water-equivalent as reported in the DICOM Dose Structured Report of 389 pediatric patients over a 2 year period (IRB 25-004864) to recommend an appropriate patient weight threshold for the best imaging technique.

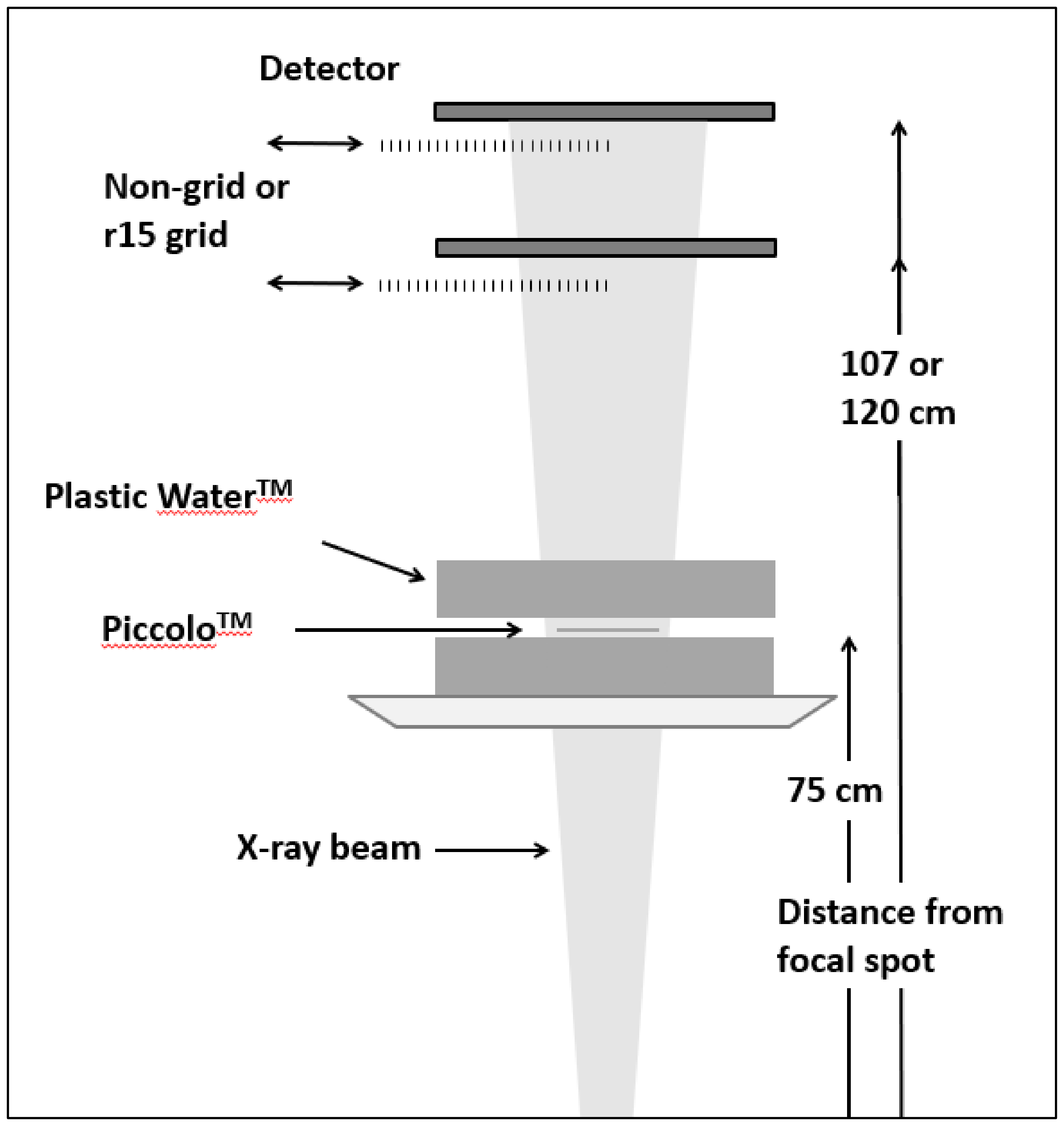

FIGURE 1. Scale line drawing of the X-ray imaging setup.

RESULTS

A 2D snr map of the Piccolo™ is shown in Fig. 2. That pixel-specific snr was lower for the fine wire body than for the radio-dense hubs is the expected result.

The influences of SID 107 vs. SID 120 cm and non-grid vs. r15 grid on Piccolo™ SNR are demonstrated in Fig. 3 as function of phantom thickness. For all phantom thicknesses, the SID 120 cm, non-grid technique provided the highest test object SNR. Results for other clinical devices and iodine disks used as test devices were similar to that presented in Fig. 3.

Figure 4 shows the relationship between patient weight and patient water equivalent thickness. The substantial variability of water equivalent thickness is due to anatomic variability and changes in X-ray projection angle.

Comparison of the data in Fig. 4 with phantom thickness 24 cm leads to a recommendation that the SID 120 cm, non-grid technique should be used for all patients who weigh less than ~60 kg.

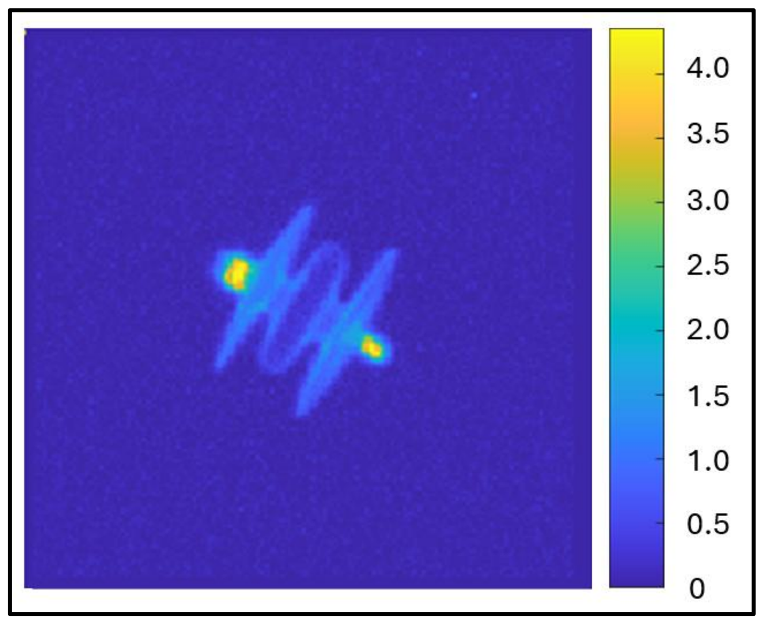

FIGURE 2: Pixel-specific *2D snr* map of the 4 mm Piccolo™.

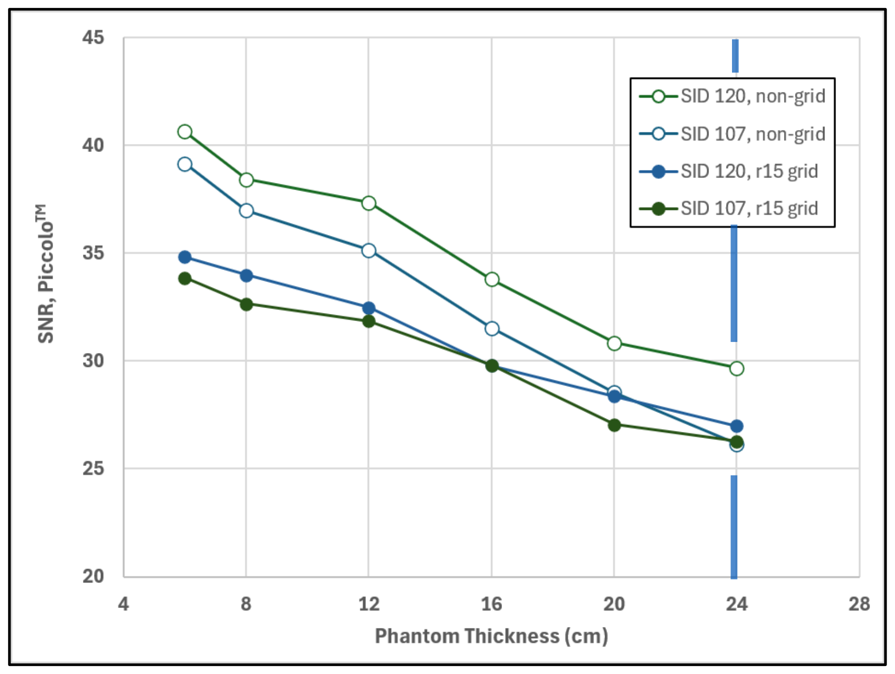

FIGURE 3. For all phantom thicknesses and with X-ray technique fixed for each thickness, the SID 120 cm, non-grid technique provided the highest PiccoloTM SNR.

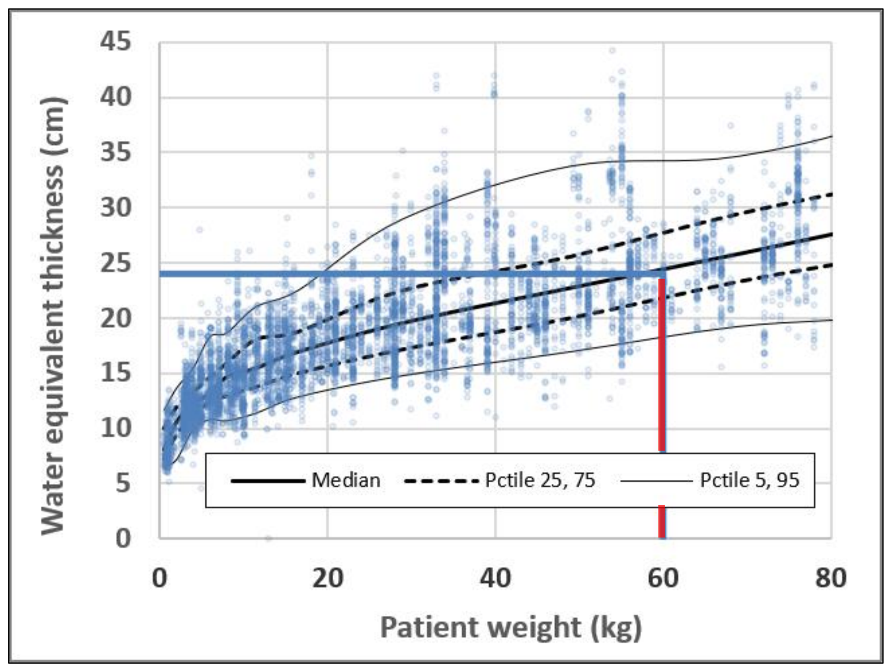

FIGURE4. Relationship between water equivalent patient thickness and patient weight. Intersection of the median patient thickness and thickness = 24 cm occurred at ~60 kg.

DISCUSSION

Why is the long SID, non-grid technique best for <60 kg patient fluoroscopy and angiography?

- Thin phantoms and patients are associated with low levels of X-ray scatter.
- The long air gap associated with SID 120 cm allows scatter to dissipate away from the detector but does adversely affect the useful primary X-ray beam.
- Introduction of an anti-scatter grid absorbs a portion of the useful primary beam and degrades SNR.
- For pediatric patients, a small 0.4 mm focal spot can be used for both fluoroscopy and angiography imaging, thus mitigating the detrimental effects of focal spot penumbral blur.

REFERENCES

1. Fetterly KA. A pixel-specific model observer for high-fidelity assessment of x-ray angiography imaging system performance. Phys Med Biol. Jun 8 2026;10.1088/1361-6560/ae79cfdoi:10.1088/1361-6560/ae79cf